Prospects for permanent magnets with non-critical rare earth elements in traction drive motors

M.J. Kramer
Ames Laboratory, Iowa State University, Ames IA 50011, USA

Jun Cui
Ames Laboratory, Iowa State University, Ames IA 50011, USA

Iver Anderson
Ames Laboratory, Iowa State University, Ames IA 50011, USA

Ikenna C. Nlebedim
Ames Laboratory, Iowa State University, Ames IA 50011, USA

It has been over a decade since the first crisis in the rare earth elements (REEs) supply chain [1]. While significant investments in exploring and developing new sources for REEs, alternatives to REE-based permanent magnets (PM), and new processing methods to reduce the more critical heavy REEs, much still needs to be done. Concern for climate change has accelerated regulations on internal combustion engines (ICE) and even planning outright bans of ICEs in many localities. Nd-Fe-B based PMs still provide the highest energy density in the temperature range (< 150°C) for most consumer and industrial applications. While current proven reserves for light REEs are sufficient in the near-term outlook for PM applications [2, 3], the supply chain for manufactures outside of China remains vulnerable. The heavy REE (Dy, Tb, Ho) needed for improved high temperature PM operations are scarce and getting scarcer [4] resulting in more uncertainty in price and availability. While there are many alternatives to the current Nd-Fe-B based PM alloys and some of these compounds can be utilized in PM-type traction motors, there is a penalty to the overall system performance. Substituting with these lower energy density alternative PMs will result in higher fossil fuel consumption in hybrid vehicles and lower driving range in all-electric vehicles for the same vehicle size. For all electric vehicles (AEV), loss in PM performance will require additional battery capacity. A 5% increase in battery capacity will cost nearly US$300, which is almost double the cost of the materials that goes into PM motors. Switching to lower performing PMs or to induction motors will greatly increase AEV [5]. This also means that the demand for the critical materials such as graphite, Li, Ni, Mn, Co will increase more rapidly.

The solutions are 1) develop a new PM without critical elements with performance matching Nd-Fe-B based PM, 2) develop new motor topologies that utilized characteristics of current non-critical PMs more efficiently, and/or 3) find ways to maintain the operating temperature performance of the Nd-Fe-B based PM without critical elements. The first scenario is unlikely in the near term because many significant large-scale research efforts, conducted since 2012, have yet to discover such new, powerful PM materials. While there have been some intriguing PM discoveries, many of these materials are far from commercial applications or even full lab demonstrations. There has also been considerable effort in new topologies for PM based motors that have been promising [6]. In fact, better integration between PM materials research and motor design is needed to foster advances in both arenas.

Most of the success has been in more efficient use of heavy REE, such as diffusing Dy only into the near surfaces of the Nd-Fe-B PMs that experiences the highest demagnetization fields [7]. Another promising route is to reduce the grain size (< 5 µm) of the Nd-Fe-B PMs to produce higher coercivity (H_{ci}) and operating temperature without heavy REE additions [8, 9]. The smaller grains are more resistant to field reversals and having more grains in a given volume hardens the overall magnet. However, reducing the grain size doesn’t improve the slope of the temperature dependence of the coercivity, it simply shifts up the whole H_{ci} (T) curve. Our initial investigations on grain size effects on the properties of heavy REE free sintered PMs has shown that even modest reductions in the grain size can result in significant improvements in H_{ci} (Figure 1). However, this work has revealed that the mode of milling, their energy inputs and mechanism for commutating particles affects particle shape and size distribution. Also critical is powder handling since particle surfaces make up a much higher fraction of the volume. Special care in handling the powders is required to keep the uncontrolled surface oxidation at a minimum.

To address this, Ames Laboratory has developed a Controlled Atmosphere Materials Processing System (CAMPS). CAMPS provides a solution for synthesis of high quality magnets in an environment that limits potential for oxidation and moisture contamination. It enables multiple complex materials synthesis operations to be performed in inert atmosphere. Within the same inert atmosphere, materials can be milled, magnetized, compacted and heat-treated. An optical microscope in the CAMPS allows for the imaging of particles during processing. One of the key enabling features of CAMPS is that the tools for the operations are in inert chambers while most of the control of the operations are performed outside of the chamber.

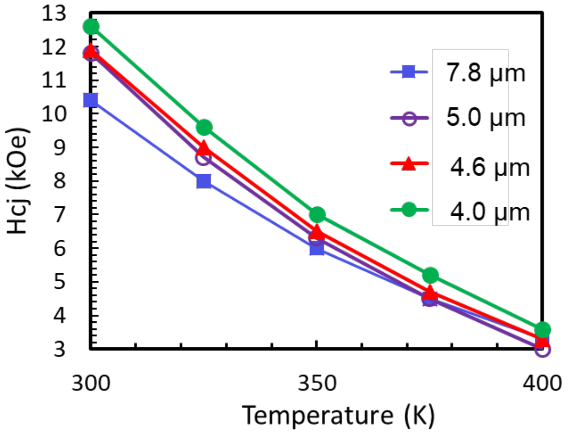

Figure 1. Effect of average grain size on the temperature dependence of the corecivity. The energy product also increased from 34.8 to 43.6 MGOe at room temperature with decreasing grain size.

The other challenge is to limit the grain growth during sintering of the superfine feedstock powder. We are investigating lower sintering temperatures, using excess REE as well as other external transient liquid phase to further reduce sintering temperature while achieving full magnet densification. Adding a grain boundary pinner may also be necessary to prevent grain growth. The extra effort in grain size reduction will be for naught if a fully dense; oxide free part that maintains the small grain size cannot be fabricated.

Non-rare earth magnets can be used for EV traction motor if the strict requirement of high power density and low cost can be met. One approach to mitigate the impact of weaker magnet on the motor density is to increase motor excitation frequency. However, this also creates other challenges. For example, at higher frequency, the hoop stress will be higher and eddy losses will be much higher in both soft and hard magnetic materials. We will present results on a recently completed project demonstrating that a 10 KW motor with power density of 1.2 KW/kg and 4.3 KW/L using MnBi PM. The motor run at 400 Hz. Its stator is made of 6.5%Si steel, which has 50% higher electrical resistivity comparing the common 3.2%Si steel. The motor maintained 90% efficiency when running at full power.

References

1) Critical Materials Strategy, U.S. DOE, http://energy.gov/sites/prod/files/edg/news/documents/criticalmaterialsstrategy.pdf, 2010
2) U.S. Geological Survey, 2020, Mineral commodity summaries 2020: U.S. Geological Survey, 200 p., https://doi.org/10.3133/mcs2020.
3) For instance see: metals-m@argusmedia.com
4) http://www.adamasintel.com/wp-content/uploads/2019/06/Adamas-Intelligence-Rare-Earths-Small-Market-Big-Necessity-Q2-2019.pdf
5) http://www.adamasintel.com/wp-content/uploads/2019/07/Adamas-Intelligence-Rare-Earths-Market-Issues-and-Outlook-Q2-2019.pdf
6) Swanke, J., Bobba, D., Jahns, T. M. & Sarlioglu, B. in 2019 IEEE Transportation Electrification Conference and Expo (ITEC). 1, DOI 10.1109/itec.2019.8790587.
7) Sepehri-Amin, H., Ohkubo, T. & Hono, K. Grain boundary structure and chemistry of Dy-diffusion processed Nd–Fe–B sintered magnets. J Appl Phys 107, 09A745, doi:10.1063/1.3351247 (2010).
8) Nothnagel P, Müller KH, Eckert D, Handstein A. The influence of particle size on the coercivity of sintered NdFeB magnets. Journal of Magnetism and Magnetic Materials. 1991 Oct 1; 101(1-3):379.
9) Sagawa, Masato. "Sintered NdFeB magnet and method for manufacturing the same." U.S. Patent No. 9,589,714. 7 Mar. 2017.

Enhancement of magnetic anisotropy of $L1_0$-FeNi nanoparticles and the related compounds for realization of rare-earth free magnet

Sho Goto[1], Eiji Watanabe[1], Yoshiaki Hayashi[1], Takahiro Nishio[1], Hiroaki Kura[1], Takashi Suemasu[2], Hideto Yanagihara[2], Eiji Kita[2], Takashi Honda[3], Keita Ito[4,5], Yusuke Shimada[4], Masahito Tsujikawa[5,6], Masaki Mizuguchi[4,5], Masafumi Shirai[5,6,7], Toyohiko Konno[4], Koki Takanashi[4,5,7]

[1] Advanced Research and Innovation Center, DENSO CORPORATION, Aichi, 470–0111, Japan.

[2] Department of Applied Physics, University of Tsukuba, Ibaraki, 305–8573, Japan.

[3] Institute of Materials Structure Science, High Energy Accelerator Research Organization, Ibaraki 305-0458, Japan

[4] Institute for Materials Research, Tohoku University, Sendai 980-8577, Japan

[5] Center for Spintronics Research Network, Tohoku University, Sendai 980-8577, Japan

[6] Research Institute of Electrical Communication, Tohoku University, Sendai 980-8577, Japan

[7] Center for Science and Innovation in Spintronics, Core Research Cluster, Tohoku University, Sendai 980-8577, Japan

In recent years, with the growing awareness of the environment, expectations for the development of high-performance motors for reducing power consumption are increasing. Especially in the automobile industry, the shift to electrified vehicles is progressing rapidly on a global scale, and the importance of high-performance motors is increasing year by year. General automobiles are equipped with more than 100 motors, including a drive main motor, and there is a demand for improved performance and cost reduction of motor products. The functions required of magnets vary depending on the intended use of the motor, such as high magnetization, high coercive force, heat resistance, and rust prevention. For products that are required high torque, such as drive main motors, strong magnets with high coercive force and high magnetization are required. In addition, heat resistance is also important because it is expected to be used under high load. On the other hand, water pumps, oil pumps, etc. are required to have rust prevention properties rather than magnetic performance. In future magnet development, not only the improvement of the maximum energy product $(BH)_{\mathrm{max}}$ of the magnet but also the variety of functions will be important.

Meanwhile, the material we focused on was $L1_0$-FeNi. $L1_0$-FeNi is a material discovered in the 1960s , which is known to be present in iron meteorites in very small amounts.1) Although $L1_0$-FeNi does not contain rare earths, its uniaxial magnetic anisotropy energy (K_u) is 1.3×10^6 J/m^3 and its saturation magnetization is 1.6 T, which is expected to be comparable to neodymium magnets. In addition, the Curie temperature of $L1_0$FeNi is said to be 550 °C or higher, so it can be expected to be used at high temperatures. A lot of studies on $L1_0$-FeNi have been made to date, 1)-7) but most of them were fundamental; the degree of order and/or the fraction of $L1_0$-phase were not enough.

Aiming at the practical application of $L1_0$-FeNi, we have developed the Nitrogen Insertion and Topotactic Extraction method (NITE) 8) as a method that can stably synthesize high-quality $L1_0$-FeNi. A schematic diagram of the NITE method is shown in Fig. 1. The long-range order parameter (S) of $L1_0$-FeNi prepared by the NITE method was $S = 0.71$, and the coercive force was 142 kA / m. This coercive force is small for application as a magnet. The small coercive force seems to be caused by crystal grains are not magnetically isolated by sintering and Ku is low. In particular, improving K_u is important from the viewpoint of securing the potential of materials.

We are trying to improve K_u of $L1_0$-FeNi by two approaches. The first approach is to improve the S. In general, K_u of $L1_0$-type ordered alloy is said to increase in proportion to the square of S.5),9) In the NITE method, the ordered structure of $L1_0$-FeNi inherits the structure of the precursor FeNiN. Therefore, in order to obtain $L1_0$-FeNi with high S, it is important that Fe and Ni are completely ordered in the state of FeNiN. Therefore, in order to understand the ordered state of FeNiN, the arrangement of Fe, Ni, and N atoms was investigated using neutron diffraction. In conclusion, it was found that FeNiN is ordered by about 100% in Fe and Ni, and N atoms are in the Fe atomic plane. It was found that the denitriding process needs to be improved as the new issue to improve the S of $L1_0$-FeNi. Another approach to improving K_u is to increase tetragonality. $L1_0$-FeNi has a c / a value is almost unity showing contrast to other $L1_0$ type ordered alloys such as FePt with 0.96 of c / a.[10)] Theoretical studies have been conducted to improve K_u if the crystals can be distorted to change c / a. In this study, we propose ordered-FeNi-N_x (x = 0 to 1) in which an arbitrary amount of nitrogen is introduced into $L1_0$-FeNi as a means for changing c / a. According to the first principles calculations, $K_u = 1.61\times10^6$ J/m^3 was obtained for c / a = 1.025 at x = 0.25, and $K_u = 1.96\times10^6$ J/m^3 for c / a = 0.992 at x = 0.5, leading to larger K_u than that of $L1_0$-FeNi. It is considered that K_u is improved by the tetragonality of the crystal structure by N-doping. The ordered-FeNi-N_x was synthesized by topotactic nitriding of $L1_0$-FeNi. As a result, the nitride had two phases with x of 0.5 and 1.0, and the nitrogen content was not continuously controlled. For x = 0.5 the crystal structure as shown in Fig. 2 is expected. From the crystal structure analysis, the lattice constants were estimated to be a = 3.78Å, c = 3.73Å, and c / a = 0.988, and we have succeeded in distorting the crystal by introducing N as theoretically expected. However, the magnetic measurement gave the coercive force of ordered-FeNi-$N_{0.5}$ much smaller than that of $L1_0$-FeNi. The reason for the discrepancy with the calculation results is currently under investigation.

In order to put $L1_0$-FeNi into practical use as a magnet, we need to work on further improving S, making crystals tetragonality, and magnetically isolating crystal grains.

Acknowledgements

This paper is based on results obtained from the Future Pioneering Program "Development of magnetic material technology for high-efficiency motors" commissioned by the New Energy and Industrial Technology Development Organization (NEDO).

Reference

1) L. Néel et al., J. Appl. Phys., 35 (1964).
2) J. F. Albertsen, et al., Nature 273 (1978) 453.
3) P. Wasilewski et al., Earth Planet. Inter., **52** (1988) 150.
4) T. Kojima et al., Jpn. J. Appl. Phys., **51** (2012) 010204.
5) Y. Miura et al., J. Phys. Condens. Matter, **25** (2013) 106005.
6) T. Mohri, J. Mater. Sci., **50** (2015) 7705.
7) A. Makino et al., Sci. Rep. **5** (2015) 16627.
8) S. Goto et al., Sci. Rep. **7** (2017) 13216.
9) S. V. Komogortsev et al., Appl. Phys. Lett. **103** (2013) 152404.
10) J. Crangle et al., J. A. Philos. Mag. **38** (1983)1.

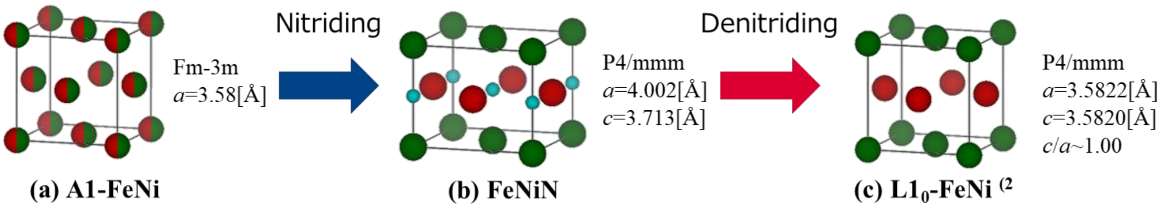

(a) A1-FeNi **(b) FeNiN** **(c) $L1_0$-FeNi** (2

Fig.1 Conceptual diagram for fabrication path of ordered FeNi alloys by NITE method Models of crystal lattices for (a) A1-FeNi, (b) FeNiN, and (c) $L1_0$-FeNi are depicted with Fe (red), Ni (green), and N (light blue) atoms. Atoms identified by red and green indicate that Fe and Ni are randomly arranged according to the ratios of colored areas.

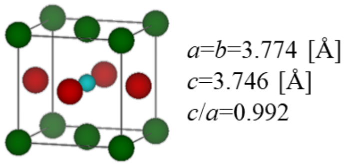

Fig.2 Crystal structure model of ordered-FeNi-$N_{0.5}$. This structure is expected to have a smaller c / a value than $L1_0$-FeNi.

Prospect of 1-12 based permanent magnets

~ Demonstration of high coercivity in thin films and current status of 1-12 bulk magnet~

[1]Y.K. Takahashi, [1]D. Ogawa, [1]H. Sepehri-Amin, [2]T. Shima, [1]T. Ohkubo, [1]S. Hirosawa, [1]K. Hono
([1]NIMS, [2]Tohoku Gakuin Univ.)

$SmFe_{12}$-based compound is one of the candidates for next generation permanent magnet due to its high saturation magnetization ($\mu_0 M_s$), high anisotropy (K) and high Curie temperature (T_c) [1]. Since $SmFe_{12}$-based compound is unstable at RT, the addition of the phase stabilizing element is necessary, which causes large reduction in magnetization. Recently, Kuno *et al.*[2] reported high $\mu_0 M_s$ by reducing Ti composition which is one of the phase stabilizing elements and substituting Fe and Sm with Co and Zr, respectively. Later, Hirayama *et al.* [3] prepared the single crystal $Sm(Fe_{0.8}Co_{0.2})_{12}$ film by sputtering and demonstrated high magnetic properties of $\mu_0 M_s$=1.78 T, H_a =12 T and T_c =859 K., which are superior to those of $Nd_2Fe_{14}B$. Even in the working temperature of the motor in electric vehicle (EV) or hybrid EV (HEV), these properties are higher than those of $Nd_2Fe_{14}B$. One drawback in $Sm(Fe_{0.8}Co_{0.2})_{12}$ compound is too low coercivity ($\mu_0 H_c$) for the permanent magnet application. In order to demonstrate the high $\mu_0 H_c$, we have controlled the microstructure by the diffusion process [4] and cosputtering of the nonmagnetic elements [5].

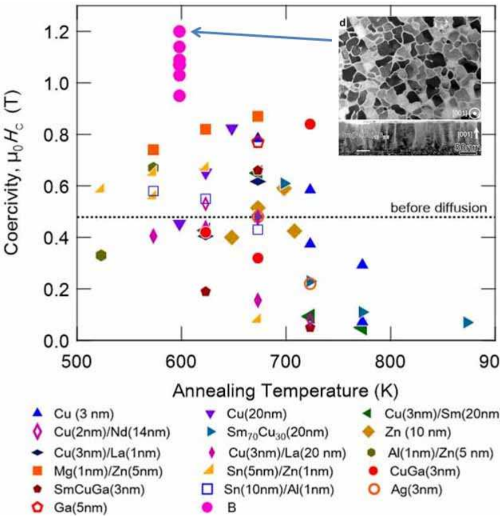

Fig. 1 Change of $\mu_0 H_c$ of the diffusion processed $Sm(Fe_{0.8}Co_{0.2})_{12}$ film as a function of annealing temperature. $\mu_0 H_c$ of the cosputtered $Sm(Fe_{0.8}Co_{0.2})_{12}$-B film is also shown.

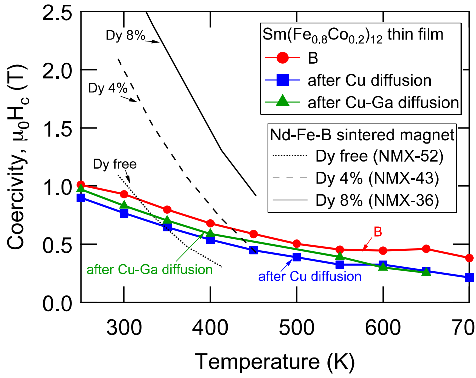

Fig. 2 Temperature dependence of $\mu_0 H_c$ in Nd-Fe-B magnets, $Sm(Fe_{0.8}Co_{0.2})_{12}$ film with Cu and Cu-Ga diffusion.

Fig. 1 shows $\mu_0 H_c$ of the diffusion processed $Sm(Fe_{0.8}Co_{0.2})_{12}$ film as a function of annealing temperature. The optimum annealing temperature ranges from 623 K to 723 K. Cu, Cu-Ga, and Mg-Zn are the effective infiltration sources for igh $\mu_0 H_c$ corresponding to 0.78 T, 0.84 T, and 0.87 T, respectively. The microstructure of Cu-Ga diffused sample shows that the Cu and Ga are diffused into the grain boundary of $Sm(Fe_{0.8}Co_{0.2})_{12}$ grains. However, Cu and Ga do not form uniform intergranular phase. It could be the reason for marginal increase of $\mu_0 H_c$. B containing sample shows the highest $\mu_0 H_c$ of 1.2 T. As shown in the in-plane and cross-sectional TEM images of the inset, it forms well-separated nanogranular microstructure with about 40 nm diameter of $Sm(Fe_{0.8}Co_{0.2})_{12}$ grains perfectly enveloped by the B-rich amorphous grain boundary phase. Because of the magnetization and anisotropy difference between $Sm(Fe_{0.8}Co_{0.2})_{12}$ grains and grain boundary phase, the highest $\mu_0 H_c$ of 1.2T was achieved. Fig. 2 shows the temperature dependence of $\mu_0 H_c$ in the $Sm(Fe_{0.8}Co_{0.2})_{12}$ films with high $\mu_0 H_c$. Those in the commercial Nd-Fe-B magnets are shown for the comparison. $Sm(Fe_{0.8}Co_{0.2})_{12}$ films with high $\mu_0 H_c$ have small absolute value of temperature coefficient of coercivity (β ~ -0.2 %/K) due to the high T_c. These results indicate that $Sm(Fe_{0.8}Co_{0.2})_{12}$ could be a superior compound for permanent magnet application compared to $Nd_2Fe_{14}B$ magnet if optimum microstructure can be achieved in bulk with high $\mu_0 H_c$. In the talk, I would review current status of the investigation for 1-12 bulk magnet.

(1)K. Ohashi *et al.*, *IEEE Trans Magn.***23**, 3101 (1987).(2)T. Kuno *et al.*, *AIP Adv.* **6** 025221 (2016). (3) Y. Hirayama *et al*, *Scr. Mater.***138**, 62 (2017). (4) D. Ogawa *et al*, Scr. Mater164, 140 (2019). (5) H. Sepehri-Amin *et al*, Acta Mater194, 337 (2020).

First-principles Study of Thermodynamic Stability in Multi-elements Alloying (Sm,X)(Fe,Y)$_{12}$Z Compounds

Saengdeejing Arkapol, Chen Ying
(School of engineering, Tohoku University)

$SmFe_{12}$-based compounds have been considered one of the most promising candidates for the next generation high performance magnetic materials. $SmFe_{12}$-based compounds exhibit excellent intrinsic hard magnetic properties with lesser amount of rare earth elements compare to other hard magnetic materials, while synthesizing $SmFe_{12}$ compounds faces a big difficulty due to the thermodynamic stability of these compounds. Additional elements doping has been attempted to stabilize $SmFe_{12}$ compounds. Ti is currently one of the best elements to thermodynamically stabilize $SmFe_{12}$ compounds but it degrades the magnetic properties. Multi-element alloying approach is generally required to achieve the desired stability while minimized the degradation of the magnetic properties. In order to understand the effect of multi-elements on the stability and magnetic properties of $SmFe_{12}$-based compounds with multi-element alloying, systematical calculations of $(Sm,X)(Fe,Y)_{12}Z$ (X=Zr/Ce, Y=Co/V/Ti, Z=B) have been conducted.

The first-principles calculations become increasingly difficult due to the complexity of the structures. The supercell with larger number of atoms to represent the correct composition and random arrangement of atoms becomes inevitable. The Special Quasirandom Structure (SQS) model is adopted to imitate the random atomic configurations. The electronic structure and total energy at 0K are calculated by DFT, the contribution of the lattice vibration at finite temperature to the free energy is obtained from Debye-Grüneisen model[1].

Several SQS for multi-elements alloying in $(Sm,X)(Fe,Y)_{12}Z$ are generated. It is found that all structures are thermodynamically stable with respect to the referent state which is consists of ground state structures of component elements. Equation of state fitting is performed on each SQS to obtain parameters required for Debye-Grüneisen model to evaluate the vibrational free energy. Figure 1 shows the SQS model(a) and calculated free energy as a function of temperature in $Sm(Fe_{0.75}V_{0.25})_{11.5}Ti_{0.5}$ (b), as an example. Different contributions to the free energies are plotted separately to illustrate the magnitude of each contribution to the free energy. It is found that most of 3d transition elements seem to stabilize the $SmFe_{12}$ structure through the vibrational contribution to the free energy in single element doping ($SmFe_{11}Y$). Increasing the concentration of alloying elements beyond $SmFe_{11}Y$ tends to destabilize the structure at the lower temperature. The contributions to the stability of $SmFe_{12}$ compound from the configurational entropy is also important in some systems such as $Sm(Fe_{0.75}Co_{0.25})_{11}V_{0.5}Ti_{0.5}$. By carefully balancing between intrinsic formation energy at 0K, vibrational contribution and configurational entropy, it is possible to design the multi-element alloying $SmFe_{12}$ compound with optimum thermodynamic stability and magnetic properties.

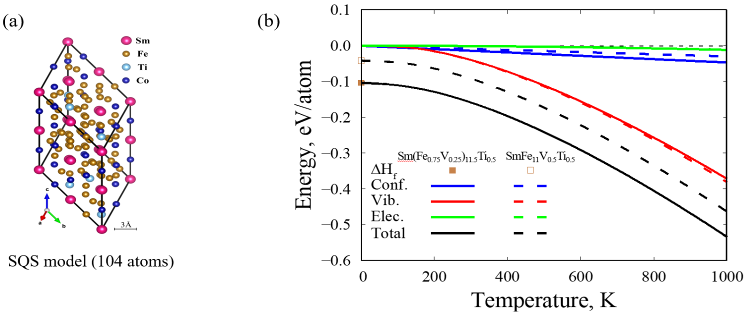

SQS model (104 atoms)

Figure 1: (a)The SQS model for random mixing of Sm $(Fe_{0.75}V_{0.25})_{11.5}Ti_{0.5}$.
(b)Free energy at temperature up to 1000K and contributions of each physical effects in $Sm(Fe_{0.75}V_{0.25})_{11.5}Ti_{0.5}$ with comparison to $SmFe_{11}V_{0.5}Ti_{0.5}$.

Reference

1) Moruzzi V.L., et al. *Phys. Rev. B* 37 (1988) 790.

Chemical Synthesis of $(Sm,Zr)(Fe,Co,Ti)_{12}$ Magnetic Mesoscopic Particles

T. T. Trinh, R. Sato and T. Teranishi
(Institute for Chemical Research, Kyoto University)

Multielement $(Sm,Zr)(Fe,Co,Ti)_{12}$ ($ThMn_{12}$, *I*4/*mmm*) compounds have the potential to meet current demands for rare-earth-element-lean permanent magnets with ultra-large energy product and operating temperatures of 150–200 °C. However, their magnets with substantial coercivities have not been realized yet despite their impressively large magnetic anisotropy field and enormous research efforts. The following critical issues make it extremely challenging to practically realize their hard magnetic potential: unoptimized particle size and shape, especially in the mesoscopic scale; introduction of inappropriate intergranular boundary phases resulted from the simultaneous formation of equilibrium ferromagnetically soft phases (e.g., Fe, Co, FeCo) along with the typical $(Sm,Zr)(Fe,Co,Ti)_{12}$ phase; difficulty in fabricating anisotropic magnets using liquid-phase sintering due to relatively high melting temperature of the compounds. Herein we present our recent achievements in the advanced chemical synthesis of ultrafine $(Sm,Zr)(Fe,Co,Ti)_{12}$ mesoscopic particles with controllable grain-size and composition. As a result, their average size of *ca.*1 μm was obtained by thermodynamic control (Fig. 1A, B). Interestingly, we could simultaneously introduce a thin Sm surface (*ca.*2 nm) (Fig. 1A), which can serve as a non-magnetic intergranular boundary. Although the resultant particles exhibited relatively low remanence and coercivity, they were highly susceptible to magnetic-field alignment (Fig. 1C), promising a high potential for the fabrication of anisotropic magnets using a rapid low-temperature current sintering method. Synthetic prospects will move a step forward in the size control through kinetics to obtain their particle size in the range below 1 μm, where an ultra-large coercivity could be achieved.

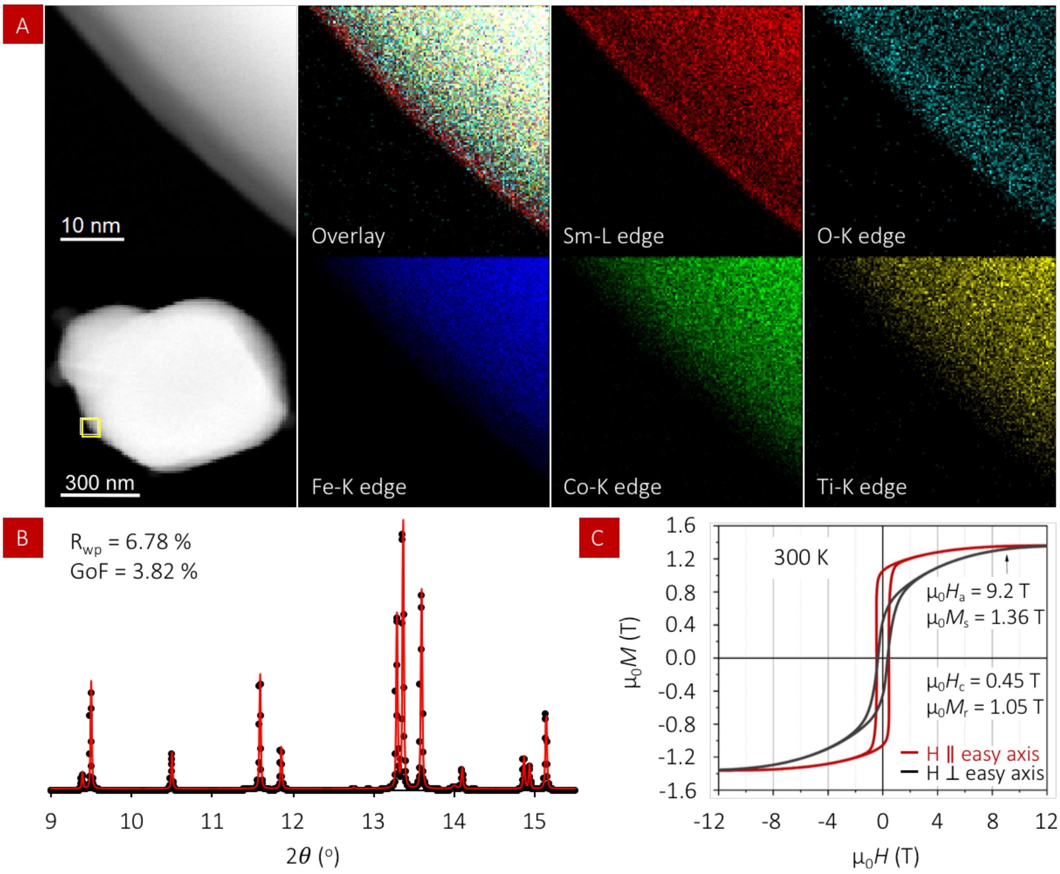

Fig. 1 Structural analysis and magnetic properties of chemically synthesized $Sm(Fe_{0.8}Co_{0.2})_{11}Ti@Sm$ core@shell mesoscopic particles: (A)HAADF and EDS elemental mapping image, (B) Rietveld refinement synchrotron XRD pattern, and (C) M–H curves.

Atomistic study of thermally-activated magnetization processes in rare earth permanent magnets

Seiji Miyashita[1,2], Masamichi Nishino[2,3], Yuta Toga[1,2], Taichi Hinokihara[1,2], Takashi Miyake[2,4], Hisazumi Akai[1,2], Satoshi Hirosawa[2], Akimasa Sakuma[5]

[1]Institute for Solid State Physics, The University of Tokyo, Kashiwa 277-8581, Japan
[2]ESICMM, National Institute for Materials Science (NIMS), Tsukuba, Ibaraki 305-0047, Japan
[3]International Center for Materials Nanoarchitectonics, NIMS, Tsukuba, Ibaraki 305-004, Japan
[4]CD-FMat, National Institute of Advanced Industrial Science and Technology (AIST), Tsukuba, Ibaraki 305-8568, Japan
[5]Department of Applied Physics, Tohoku University, Sendai 980-8579, Japan

For practical use of magnets, in particular at high temperatures, it is very important to study temperature dependence of magnetic properties [1,2]. We present our trials on this problem for the high-performance $Nd_2Fe_{14}B$ magnets (Fig.1). For this purpose, first we constructed an atomistic Hamiltonian to properly take into account the temperature [3]. With it, we calculated various thermodynamic quantities by methods of statistical physics, e.g., a constrained Monte Carlo method [3] and a stochastic LLG equation [4]. We confirmed that temperature dependences of the magnetization and anisotropy energies well reproduce the corresponding experimental results (Figs.2) [3]. Moreover, microscopic properties, e.g. the domain wall profiles [5], anisotropy of the exchange coupling constant reflecting the crystal structure [6], and also dynamical properties, e.g., the spectrum of FMR (ferromagnetic resonance) [7] were also studied. As a merit of the atomistic model, we can find atom-specific ordering properties [3].

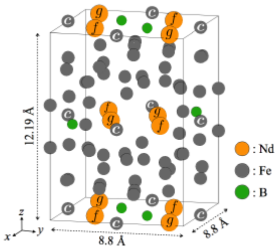

Fig.1 Unit cell of $Nd_2Fe_{14}B$

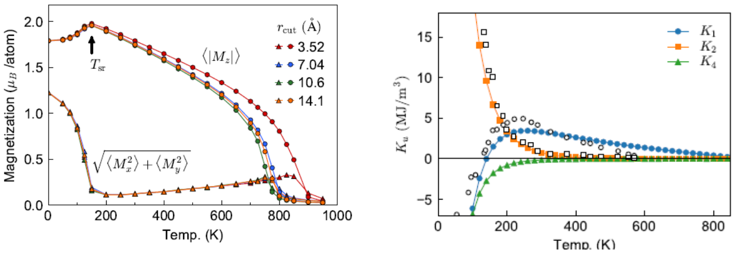

Fig.2 Temperature dependence of magnetization and anisotropy constants [3].

The most important property of magnets is the coercivity. However, in contrast to the above-mentioned thermodynamic quantities, we do not have theoretical formula for the coercivity, and thus so far only little study has been done on quantitative estimation of the coercivity at finite temperatures. We studied this problem in nano-size grains by a method using the free-energy landscape obtained by Wang-Landau method [8], and also by a direct dynamical simulation of the stochastic LLG equation [9]. There, the strength of magnetic field at which the relaxation time of the magnetization reversal is 1second (a definition of coercivity) and its temperature dependence are obtained.

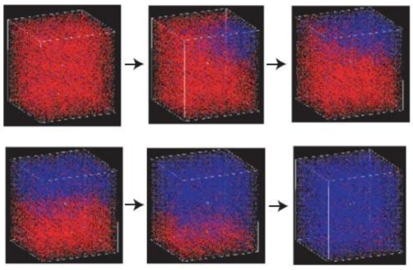

Fig.3 Magnetization reversal in a nano grain [9]

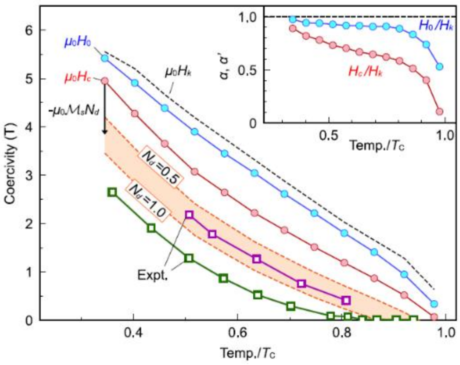

Fig. 4 Temperature dependences of coercivities [8]

It was found that the coercivity at a high temperature (about half of the critical temperature) is around 3T which is the theoretical maximum value although it is significantly reduced from the one at zero temperature. For larger grains, the dipole-dipole interaction plays a role [10] and the multidomain magnetic structure appears [11]. We also discuss a mechanism of coercivity in such cases. Real magnets consist of hard magnet ($Nd_2Fe_{14}B$) grains each of which are covered by grain boundary material. Thus, it is important to study how the boundary phases affect the coercivity [12], which is also presented. Finally, ensemble effects of gains on the coercivity are also reported from a viewpoint of the first-order reversal curves (FORC).

[1] S. Hirosawa, M. Nishino, S. Miyashita, Adv. Nat. Sci.: Nanosci. Nanotechnol. **8**, 013002 (2017).

[2] S. Miyashita, M. Nishino, Y. Toga, T. Hinokihara, T. Miyake, S. Hirosawa and A. Sakuma, Scripta Materialia, **154**,259 (2018).

[3] Y. Toga, M. Matsumoto, S. Miyashita, H. Akai, S. Doi, T. Miyake, and A. Sakuma: Phys. Rev. B 94, 174433 (2016). & Phys. Rev. B **94**, 219901 (2016).

[4] M. Nishino and S. Miyashita, Phys. Rev. B**91**, 134411(1-13) (2015).

[5] M. Nishino, Y. Toga, S. M., H. Akai, A. Sakuma, and S. Hirosawa, Phys. Rev. B **95**, 094429 (2017).

[6] Y. Toga, M. Nishino, S. Miyashita, T. Miyake, and A. Sakuma, Phys. Rev. B **98**, 054418 (2018) .

[7] M. Nishino, S. Miyashita: Phys. Rev. B **100**, 020403(R) (2019).

[8] Y. Toga, S. Miyashita, A. Sakuma and T. Miyake, npj Computational Materials **6**, 67 (2020).

[9] M. Nishino, I. E. Uysal, T. Hinokihara, and S. Miyashita, Phys. Rev. B **102**, 020413(R) (2020).

[10] T. Hinokihara, M. Nishino, Y. Toga, and S. Miyashita, Phys. Rev. B97, 104427 (2018).

[11] T. Hinokihara and S. Miyashita, arXive:2009.11574

[12] I. E. Uysal, M. Nishino, S. Miyashita, Phys. Rev. B **101**,094421 (2020).

[13] M. Nishino, I. E. Uysal , T. Hinokihara S. Miyashita, arXive:2009.08572

Nd-Fe-B 磁石の保磁力に対する表面 Nd の磁気異方性の効果

西野正理 [1]、Ismail Enes Uysal[1]、宮下精二 [2,1]
（[1] 物材機構、[2] 東大物性研）

The effect of the surface magnetic anisotropy of Nd atoms on the coercivity in Nd-Fe-B magnets

Masamichi Nishino[1], Ismail Enes Uysal[1], and Seiji Miyashita[2,1]
([1]NIMS, [2]ISSP, Univ. of Tokyo)

イントロダクション

ネオジム磁石 N-Fe-B は高い保磁力を持ち、モーターや発電機などに利用されている。新規磁石材料設計には保磁力の機構解明が重要であるが、依然として未解明の部分が多い[1]。保磁力機構の微視的なスケールからの解明には、原子論に基づくモデル化とそのダイナミクスの解析が必要である。我々は、連続体モデルによるマイクロマグネティクス計算とは異なる方法論、すなわち、結晶格子を反映した原子論的スピンモデルを用いた方法論によるネオジム磁石の磁化反転解析を行ってきた[2]。保磁力制御のためには、磁気グレインの表面、界面の性質を知ることが重要である[1,3]。第一原理計算の研究において、(001)表面の Nd 原子の異方性はバルクにおける c 軸の容易軸とは異なり、 c 面が容易面となることで保磁力の低下の原因となり得るという報告がなされた[4]。我々は、表面の Nd 原子の磁気異方性に注目して、ゼロ温度と有限温度において、表面の異方性が保磁力にどのような影響を与えるかについて調べた[5]。

磁化反転における表面の効果

磁化ダイナミクスを記述する基礎方程式である Landau-Lifshitz-Gilbert(LLG)方程式に熱揺らぎの効果を取り込んだ方法論（Stochastic LLG 法[2]）をこの系に適用して解析を行った。原子論的モデルのミクロなパラメータは、主として第一原理計から見積もった値を用いている。図 1 のように(001)面の表面 Nd 層の n 層目までの Nd 原子に対する異方性を修飾して、その効果が反転磁場に与える効果を調べた。表面 Nd 原子の異方性の修飾の仕方として、（1）磁気異方性が無い、（2）容易面を持つ、(3)強化した容易軸異方性を持つ、それぞの場合について調べた。ゼロ温度では表面一層(n=1)のみ修飾しても反転磁場は大きく変化するが、室温付近では殆ど効かず、効果が現れるには数層の修飾が必要であることが分かった。同様に(100)面における表面効果についても調べ、比較した。本公演では、3 つの修飾の仕方に対して、表面の種類、温度、修飾層の深さといった因子が保磁力に及ぼす影響について議論する。

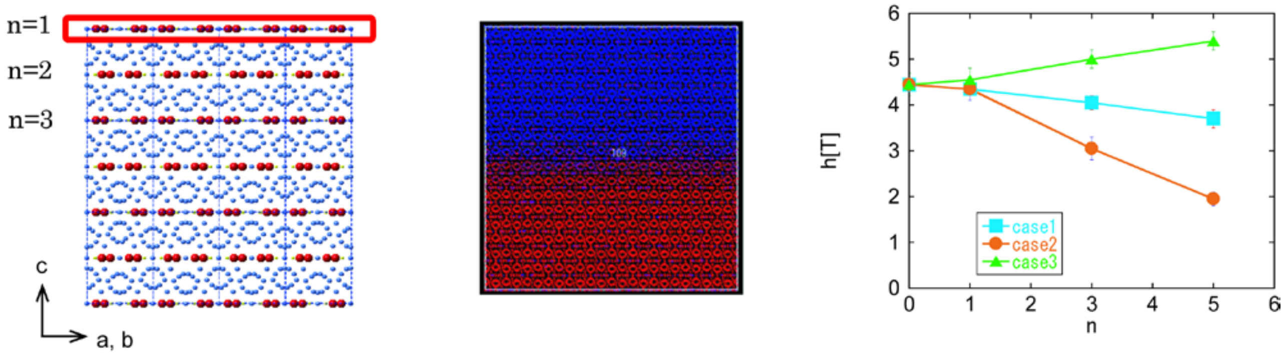

図1（左）(001)面におけるnの定義、（中）磁化反転の様子、（右）室温付近でのnに対する保磁力の変化。

参考文献

1) S. Hirosawa, M. Nishino and S. Miyashita, Adv. Nat. Sci.: Nanosci. Nanotechnol. 8, 013002 (2017).
2) M. Nishino, I. E. Uysal, T. Hinokihara, and S. Miyashita, Phys. Rev. B 102, 020413(R) (2020).
3) I. E. Uysal, M. Nishino, and S. Miyashita, Phys. Rev. B 101, 094421 (2020).
4) H. Moriya, H. Tsuchiura, and A. Sakuma, J. Appl. Phys. 105, 07A740 (2009).
5) M. Nishino, I. E. Uysal, and S. Miyashita, submitted. arXiv:2009.08572.

Observation of the demagnetization process of HDDR Nd-Fe-B sintered magnets by soft X-ray magnetic circular dichroism microscopy

A. Martin-Cid[1,2], T. Kawahara[3], S. Kobayashi[1,2], K. Toyoki[1,2], D. Billington[1,2], Y. Kotani[1], H. Kubo[3], Y. Une[3], T. Iriyama[3], M. Sagawa[3], T. Nakamura[1,2,4]
[1] Japan Synchrotron Radiation Research Institute (JASRI), 1-1-1 Kouto, Sayo 679-5198, Japan
[2] Elements Strategy Initiative Center for Magnetic Materials (ESICMM), National Institute for Materials Science, Tsukuba 305-0047, Japan
[3] Daido corporate research and development center, Daido steel Co., Ltd., 2-30 Daido-cho, Minami-ku, Nagoya 457-8545, Japan
[4] International Center for Synchrotron Radiation Innovation Smart, Tohoku University, Sendai 980-8577, Japan

Nd-Fe-B based magnets have dominated the high-performance permanent magnet market since their development in 1984. Among other applications, wind turbines and motors for electric-powered cars have experienced rapid growth due to the necessity to reduce the dependence on fossil fuels. Magnets used in these applications have to sustain high demagnetization fields under temperatures up to 200 °C, and so, as the temperature coefficient of coercivity of Nd-Fe-B magnets is large, a high coercivity (μ_0H_c ~ 3.0 T) at room temperature (RT) is needed. As Nd-Fe-B sintered magnets present a relatively low coercivity (μ_0H_c ~ 1.2 T) at RT, partial substitution of Nd with heavy rare earth (HRE) elements such as Dy or Tb is commonly used to improve the coercivity and thermal stability. In the attempt to reduce the use of the very scarce HRE, efforts are being made to improve the coercivity of HRE-free Nd-Fe-B sintered magnets by tuning the microstructure reducing the grain size of the main $Nd_2Fe_{14}B$ phase and improving the grain boundary phase of the sintered magnet. To obtain grain sizes below 1 µm, the hydrogenation-disproportionation-desorption-recombination (HDDR) and hydrogen decrepitation processes have been explored. Recently, Xu *et al.* [1] reported an unexpectedly low coercivity, of just 1.3 T, in sintered magnets with ultrafine grain sizes obtained by HDDR and the pressless sintering process (PLP) compared to those made from He jet-milling and PLP, with a coercivity of 2.14 T, while both had a similar particle size of ~1 µm. They found that HDDR processed PLP magnets presented a thinner grain boundary together with a lower concentration of non-magnetic elements in the grain boundary, which would promote the propagation of the reversal magnetic domains, and thus, reduce the coercivity.

To gain a deeper insight into the reason for the diminished coercivity on HDDR processed PLP magnets, in this work, we have analyzed the evolution of the magnetic domains on the fractured surface of four types of Nd-Fe-B-based magnets with different sizes of grains by soft X-ray magnetic circular dichroism (XMCD) microscopy. These include a hot deformed magnet with plate-like grains of ~0.37 µm with a thickness of ~100 nm in the c-axis direction, and three PLP magnets obtained from a N_2 jet-milled powder (~3 µm), a He jet-milled powder (~1 µm), and a HDDR powder (~0.8 µm), which is made by both HDDR and He jet-milling. The XMCD microscopy showed that, while the 3µm, the 1µm, and the hot deformed magnet demagnetization processes were mainly driven by nucleation and propagation of the reversal domains with a preference for the domain propagation in the hot deformed magnet, in the HDDR processed magnet, the nucleation of magnetic reversal domains dominates throughout the whole demagnetization process. Moreover, the nucleation field for the HDDR processed magnet is greatly reduced compared to the other magnets studied.

References

1) X.D. Xu *et al.*, Acta Mater. 151 (2018) 293–300.

Hysteresis design of magnetic materials for efficient energy conversion

Oliver Gutfleisch

Material Science, Technical University Darmstadt, D-64287 Darmstadt, Germany

Abstract

Magnets are key components of energy-related technologies, such as direct drive wind turbines and e-mobility. They are also important in robotics and automatisation, sensors, actuators, and information technology. The magnetocaloric effect (MCE) is of strong interest for new and disruptive solid state-based refrigeration. Magnetic hysteresis – and its inherent energy product - characterises the performance of all magnetic materials. Despite considerable progress in the modelling, characterisation and synthesis of magnetic materials, hysteresis is a long-studied phenomenon that is still far from being completely understood. Discrepancies between intrinsic and extrinsic magnetic properties remain an open challenge and magnets do not operate yet at their physical limits. The design of hysteresis for the magnets for the above applications requires an expanded detailed knowledge on different length scales. Ultimately, new strategies for effective magnetic hardening mechanisms of permanent magnets resisting high external magnetic fields and temperatures and for strong thermomagnetic responses in low fields of magnetocaloric materials are needed.
In this context, I will introduce our newly established DFG Cooperate Research Center 270 Hommage Hysteresis Design of Magnetic Materials for Efficient Energy Conversion https://www.tu-darmstadt.de/sfb270.

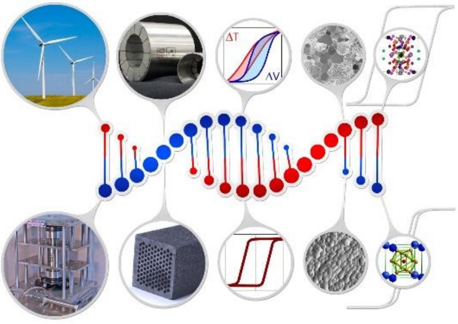

©FunctionalMaterials

[1] O. Gutfleisch, M. A. Willard, E. Brück, C. H. Chen, S. G. Sankar, and J. P. Liu, Magnetic materials and devices for the 21st century: stronger, lighter, and more energy efficient. Adv. Mater. 23 (2011) 82.
[2] K.P. Skokov and O. Gutfleisch, Heavy rare earth free, free rare earth and rare earth free magnets - vision and reality, Scripta Materialia View Point Set, 154 (2018) 289-294.
[3] T. Gottschall, A. Gracia-Condal, M. Fries, A. Taubel, L. Pfeuffer, L. Manosa, A. Planes, K.P. Skokov, O. Gutfleisch, A multicaloric cooling cycle that exploits thermal hysteresis, Nature Materials (2018).
[4] M. Duerrschnabel, M. Yi, K. Uestuener, M. Liesegang, M. Katter, H.-J. Kleebe, B. Xu, O. Gutfleisch, L. Molina-Luna, Atomic structure and domain wall pinning in samarium -cobalt based permanent magnets, Nature Communications 8:54 (2017).
[5] J. Liu, T. Gottschall, K.P. Skokov, J.D. Moore, O. Gutfleisch, Giant magnetocaloric effect driven by structural transition, Nature Mat. 11 (2012) 620.
[6] O. Gutfleisch, T. Gottschall, M. Fries, D. Benke, I. Radulov, K. P. Skokov, H. Wende, M. Gruner, M. Acet, P. Entel and M. Farle, Mastering hysteresis in magnetocaloric materials, Phil. Trans. R. Soc. A 374 (2016) 20150308.

Visualization of the magnetization reversal processes in He jet-milled Nd-Fe-B sintered magnet by X-ray magnetic tomography

M Suzuki[1], M. Takeuchi[2], S. Kobayashi[1,3], R. Haga[2], Y. Kotani[1], T. Nakamura[1,3,4], N. Kikuchi[2], T. Sasaki[3,5], T. Ohkubo[3,5], Y. Une[6], and S. Okamoto[2,3]
[1]Japan Synchrotron Radiation Research Institute, 1-1-1 Kouto, Sayo, 679-5198, Japan.
[2]IMRAM Tohoku University, Sendai 980-8577, Japan
[3]Elements Strategy Initiative Center for Magnetic Materials, NIMS, Tsukuba 305-0047, Japan.
[4]International Center for Synchrotron Radiation Innovation Smart, Tohoku University, Sendai 980-8577, Japan
[5]Research Center for Magnetic and Spintronics Materials, NIMS, Tsukuba 305-0047, Japan.
[6]Daido Corporate Research and Development Center, Steel Co., Ltd., Nagoya 457-8545, Japan

Introduction

The magnetic properties of Nd-Fe-B sintered magnets are closely related to the microstructure. To unveil the mechanism of the high coercivity emerged, the nucleation and evolution processes of reversed magnetic domains need to be clarified concerning the microstructure of a sintered magnet. Magnetic domain observation under an external magnetic field has so far been performed using Kerr microscopy and soft-X-ray scanning XMCD microscopy [1-4]. However, these existing techniques are limited to observe the domain structure on the surface of the sample, and it was not possible to investigate the magnetization reversal process inside bulk magnets. In this study, we used a recently developed hard X-ray magnetic tomography technique [5, 6] to directly observe the internal magnetic domain structure of Nd-Fe-B sintered magnets in a three-dimensional (3D) manner.

Experiment

Anisotropic Nd-Fe-B sintered magnet with an averaged particle diameter of 1 μm was prepared by the He-jet mill and pressless process [7]. A bulk specimen (remanent magnetization 1.5 T and coercivity 1.4 T) was micro-fabricated into a square column of $20\times20\times57$ μm^3 by a focused ion beam (FIB) method. A first order reversal curve (FORC) measurement was performed for another cutting sample with the same aspect ratio and larger dimensions, and it was confirmed that the FIB process has given little damage and the magnetic properties of the sample were almost unchanged. The hard X-ray magnetic microtomography experiment at the Nd L_2 edge (6.725 keV) was carried out at BL39XU of SPring-8 [5, 6]. The application of magnetic fields to the sample was performed off-line, and the magnetic domain structure of the remanent magnetization state at zero fields was observed by the X-ray tomography measurements.

Results

The formation and reversal process of the magnetic domains inside the bulk Nd-Fe-B sample was successfully observed in 3D. The widths of magnetic domains are comparable to the particle diameter, suggesting that the magnetization reversal of each particle has been visualized. Some inner grains are found to reverse independently. Thus, the nucleation points of magnetization reversal are directly demonstrated. In this talk, the correlation between the sintered microstructure and the magnetic domain structure will be discussed.

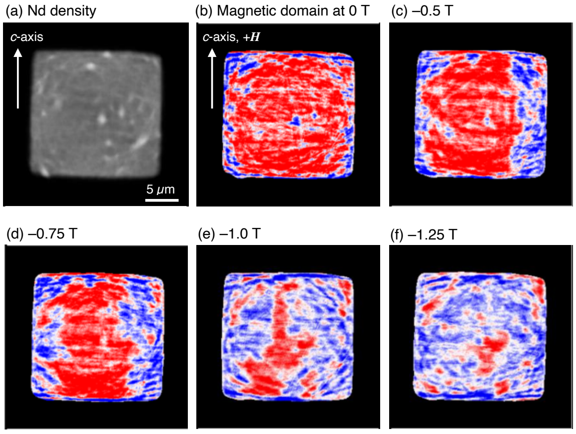

Fig. 1 Tomographic reconstructions of He-jet milled Nd-Fe-B sintered magnet. Cross sections of a square column sample at a plane parallel to the c-axis are shown.

Part of this work is supported by ESICMM under the outsourcing project of MEXT (JPMXP0112101004).

[1] M. Suzuki *et al.*, Acta Mater. **106**, 155 (2016). [2] Y. Kotani *et al.*, J. Synchrotron Rad. **25**, 1444 (2018). [3] D. Billington *et al.*, Phys. Rev. Mater. **2**, 104413 (2018). [4] S. Okamoto *et al.*, Acta Mater. **178**, 90 (2019). [5] M. Suzuki *et al.*, Appl. Phys. Express **11**, 036601 (2018). [6] M. Suzuki *et al.*, Synchrotron Rad. News **33**, 4 (2020). [7] Y. Une *et al.*, J. Jpn Inst. Met. **76**, 12 (2012).

Spins in Low-dimensional Materials Systems: Transport, Gate-control and Conversion

Masashi Shiraishi
(Department of Electronic Science and Engineering, Kyoto University, Japan)

Transport, control and conversion of spins in condensed matters have been pivotal concepts in spintronics. Spin transport is the most fundamental concept to realize spin-dependent phenomena, spin control mainly by gating enables information switching using a spin degree of freedom, and spin conversion allows detection of spins, a dissipative physical quantity. Whilst bulk metallic and semiconducting systems have been to date major material stages to realize the aforementioned concepts, low-dimensional materials systems such as atomically-flat two-dimensional materials [1-3], two-dimensional electron gases formed at an interface of a heterostructure [4,5], topologically-protected Dirac surface states in topological insulators [6,7] and ultrathin films [8] are becoming attractive materials stages to pursue novel spintronic concepts and phenomena. I will introduce the attractiveness of these new materials systems, cover an overview of the central achievements, and focus on recent investigation to pioneer novel spintronic physics in the low-dimensional materials systems.

Reference

1) B. Raes, S.O. Valenzuela et al., “Determination of the spin-lifetime anisotropy in graphene using oblique spin precession”, *Nature Commun.* 7, 11444 (2016).
2) S. Dushenko, M. Shiraishi et al., “Gate-tunable spin-charge conversion and the role of spin-orbit interaction in graphene”, *Phys. Rev. Lett.* 116, 166102 (2016).
3) A.W. Cummings, S. Roche et al., “Giant spin lifetime anisotropy in graphene induced by proximity effects”, *Phys. Rev. Lett.* 119, 206601 (2017).
4) R. Ohshima, M. Shiraishi et al., “Strong evidence for d-electron spin transport at room temperature at a $LaAlO_3/SrTiO_3$ interface”, *Nature Mater.* 16, 609 (2017).
5) E. Lesne, M. Bibes et al., “Highly efficient and tunable spin-to-charge conversion through Rashba coupling at oxide interface”, *Nature Mater.* 15, 1261 (2016).
6) Y. Shiomi, E. Saitoh et al., Spin-electricity conversion induced by spin injection into topological insulators”, *Phys. Rev. Lett.* 113, 196601 (2014).
7) Yuichiro Ando, M. Shiraishi et al., “Electrical detection of the spin polarization due to charge flow in the surface state of the topological insulator $Bi_{1.5}Sb_{0.5}Te_{1.7}Se_{1.3}$”, *Nano Lett.* 14, 6226 (2014).
8) S. Dushenko, M. Shiraishi et al., “Tunable inverse spin Hall effect in nanometer-thick platinum films by ionic gating”, Nature Commun. 9, 3118 (2018).